

FBSDE based neural network algorithms for high-dimensional quasilinear parabolic PDEs

Wenzhong Zhang*

Wei Cai[†]

June 24, 2022

Summary

In this paper, we propose forward and backward stochastic differential equations (FBSDEs) based deep neural network (DNN) learning algorithms for the solution of high dimensional quasilinear parabolic partial differential equations (PDEs). The algorithms relies on a learning process by minimizing the path-wise difference of two discrete stochastic processes, which are defined by the time discretization of the FBSDEs and the DNN representation of the PDE solutions, respectively. The proposed algorithms demonstrate a convergence for a 100-dimensional Black–Scholes–Barenblatt equation at a rate similar to that of the Euler–Maruyama discretization of the FBSDEs.

1 Introduction

The relation between stochastic processes and the solution of partial differential equations represents one of the high achievements of probability theory in the potential theory research [1], represented by the celebrated Feynman–Kac formula in linear parabolic and elliptic PDEs as a result of the Kolmogorov backward equation for the generator of the stochastic process for the former [2] and Dynkin formula for the latter [3]. The recent work by Pardoux–Peng [4] has extended the concept of classic linear Feynman–Kac formula to a nonlinear version, which connects the solution of a quasilinear parabolic PDE to a coupled pair of forward and backward

*Department of Mathematics, Southern Methodist University, Dallas, TX 75275.

[†]Corresponding author, Department of Mathematics, Southern Methodist University, Dallas, TX 75275(cai@smu.edu).

stochastic processes. This extraordinary development has made much impact in the mathematical finance in option pricing [5].

Meanwhile, in the field of scientific computing, this connection has inspired a new approach of solving high dimensional parabolic partial differential equations (PDEs) which are ubiquitous in material sciences such as the Allen–Cahn equations for phase transitions, and quantum mechanics such as Schrodinger equations as well as option pricing such as the Black–Scholes equations. For PDEs in high dimensions, the main challenge of the traditional numerical methods, such as finite element, finite difference and spectral methods, is the issue of curse of dimensionality, namely, the number of unknowns in the discretized systems for the PDEs grows exponentially in terms of the dimension of the problem. Recently, machine learning approaches based on the deep neural network have taken advantage of the Pardoux–Peng’s theory for forward and backward stochastic differential equations (FBSDEs) and PDEs. The solution to the PDEs is learned by sampling the paths of involved stochastic processes, which are discretized in time by the classic Euler–Maruyama scheme [6]. The first such an attempt was done in the work of [7], where neural network was used as an approximator to the gradient of the PDEs solutions, while the PDE’s solution follows the dynamics of the FBSDEs, and the learning was carried out by imposing the terminal condition provided by the parabolic PDEs. Another approach [8] is to approximate the PDE’s solution itself by a deep neural network, which also provides the gradient of the solution as required by the FBSDEs, the learning is then carried out by minimizing the difference between the solution given by the discretized SDEs and that given by the DNN at all discretization time stations. In this paper, an improved learning scheme will be proposed based on a similar approach in [8] but with more mathematical consistence and reasoning for the learning processes, which will provide improved convergence for the PDEs’ solutions.

The rest of the paper is organized as follows. In Section 2, we will review the Pardoux–Peng’s theory which establishes the relation between FBSDEs and quasilinear parabolic PDEs, with an emphasis on the relation between the classic Feynman–Kac formula and the nonlinear version represented by the Pardoux–Peng theory. Section 3 will first review the basic algorithm as proposed in [8], and then two new improved methods will be proposed. Section 4 will present some numerical results of the new schemes for solving a 100-dimensional Black–Scholes–Barenblatt equation. Finally, a conclusion will be given in Section 5.

2 Pardoux–Peng theory on FBSDEs and quasilinear parabolic PDEs

In this paper, we consider the scalar solution $u(t, x)$, $t \in [0, T]$, $x \in \mathbb{R}^d$ for the following d -dimensional parabolic PDE

$$u_t + \frac{1}{2} \text{Tr}[\sigma \sigma^T \nabla \nabla u] + \mu \cdot \nabla u = \phi, \quad (1)$$

with the terminal condition

$$u(T, x) = g(x), \quad (2)$$

where $\sigma = \sigma(t, x, u)$, $\phi = \phi(t, x, u, \nabla u)$, $\mu = \mu(t, x, u, \nabla u)$ are functions with dimensions $d \times d$, 1 and d , respectively. We are interested in finding the initial value $u(0, \xi)$ given $\xi \in \mathbb{R}^d$. Therefore, in some sense our problem is similar to an inverse problem for the initial data at $t = 0$.

Following Pardoux–Peng in [4], under certain regularity conditions, the forward-backward SDE reformulation gives a nonlinear implicit Feynman–Kac formula for the solution of the parabolic PDE (1). The FBSDEs are proposed as follows. Let $W_t = (W_t^1, \dots, W_t^d)$ where each W_t^j is a standard Brownian motion. Let $\{\mathcal{F}_t : 0 \leq t \leq T\}$ be its natural filtration on the time interval $[0, T]$. Then, we have the equations of stochastic processes X_t , Y_t and Z_t in d , 1 and d dimensions that are adaptive to the filtration $\{\mathcal{F}_t : 0 \leq t \leq T\}$, respectively,

$$\begin{aligned} dX_t &= \mu(t, X_t, Y_t, Z_t)dt + \sigma(t, X_t, Y_t)dW_t, \\ X_0 &= \xi, \end{aligned} \quad (3)$$

$$\begin{aligned} dY_t &= \phi(t, X_t, Y_t, Z_t)dt + Z_t^T \sigma(t, X_t, Y_t)dW_t, \\ Y_T &= g(X_T). \end{aligned} \quad (4)$$

If μ and σ do not explicitly depend on Y_t or Z_t , the FBSDEs are called *decoupled*.

We can easily show that

$$Y_t = u(t, X_t), \quad Z_t = \nabla u(t, X_t) \quad (5)$$

in fact satisfy the above equations (3) (4). By using the Ito's formula [3] and the

forward SDE of X_t , we have

$$\begin{aligned}
dY_t &= du(t, X_t) = \partial_t u dt + \nabla u \cdot dX_t + \frac{1}{2} \sum_{i=1}^d \sum_{j=1}^d \partial_{ij} u d[X^i, X^j]_t \\
&= \partial_t u dt + \nabla u \cdot (\mu dt + \sigma \cdot dW_t) + \frac{1}{2} \text{Tr}[\sigma \sigma^T \nabla \nabla u] dt \\
&= \left(\partial_t u + \nabla u \cdot \mu + \frac{1}{2} \text{Tr}[\sigma \sigma^T \nabla \nabla u] \right) dt + Z_t^T \sigma dW_t,
\end{aligned} \tag{6}$$

which gives the PDE (1) by comparing (6) with the backward SDE (4) for Y_t .

The determination of the third stochastic process Z_t from the two SDEs in (3) and (4) makes use of the martingale representation theory. Consider the following special case of the backward SDE (4) as an example:

$$Y_t + \int_t^T f(s, X_s) ds + \int_t^T Z_s \cdot dW_s = g(X_T), \quad 0 \leq t \leq T, \tag{7}$$

i.e. $\mu(t, x, u, \nabla u) = f(t, x)$, and $\sigma(t, x, u) = I_{d \times d}$ is the identity matrix. By taking the conditional expectation with respect to \mathcal{F}_t , we have

$$Y_t = \mathbb{E}[Y_t | \mathcal{F}_t] = \mathbb{E} \left[g(X_T) - \int_t^T f(s, X_s) ds \middle| \mathcal{F}_t \right], \quad 0 \leq t \leq T. \tag{8}$$

Next, we define the following martingale

$$L_t = \mathbb{E} \left[g(X_T) - \int_0^T f(s, X_s) ds \middle| \mathcal{F}_t \right], \quad 0 \leq t \leq T, \tag{9}$$

where $L_0 = Y_0$. By the martingale representation theorem [9], there exists Z_t^* such that

$$L_t = Y_0 + \int_0^t Z_s^* \cdot dW_s, \quad 0 \leq t \leq T. \tag{10}$$

The stochastic process Z_t^* is unique in the sense that

$$\int_0^T \|Z_t^* - Z_t^*\|^2 dt = 0, \quad \text{a.s.} \tag{11}$$

if Z_t^* satisfies the same condition (10) as Z_t^* [9].

Meanwhile, we can show that $Z_t = Z_t^\star$ solves the backward SDE (7),

$$\begin{aligned}
& Y_t + \int_t^T f(s, X_s) ds + \int_t^T Z_s^\star \cdot dW_s - g(X_T) \\
&= \mathbb{E} \left[g(X_T) - \int_t^T f(s, X_s) ds \middle| \mathcal{F}_t \right] \\
&\quad + \left(\int_0^T - \int_0^t \right) f(s, X_s) ds + (L_T - L_t) - g(X_T) \\
&= \int_0^T f(s, X_s) ds + L_T - g(X_T) \\
&= L_T - \mathbb{E} \left[g(X_T) - \int_0^T f(s) ds \middle| \mathcal{F}_T \right] \\
&= 0.
\end{aligned}$$

Connection with the classic Feynman–Kac formula is interpreted as follows. If in the parabolic PDE (1), ϕ has linear dependence on u , i.e.

$$\phi(t, x, u, \nabla u) = c(t, x)u(t, x) + f(t, x), \quad (12)$$

then the backward SDE (4) has an explicit solution

$$\begin{aligned}
Y_t &= e^{-\int_t^T c(s, X_s) ds} g(X_T) - \int_t^T e^{-\int_t^s c(\tau, X_\tau) d\tau} f(s, X_s) ds \\
&\quad - \int_t^T e^{-\int_t^s c(\tau, X_\tau) d\tau} Z_s^T \sigma(s, X_s, Y_s) dW_s.
\end{aligned} \quad (13)$$

By taking the conditional expectation on both sides, we arrive

$$Y_t = \mathbb{E} \left[e^{-\int_t^T c(s, X_s) ds} g(X_T) - \int_t^T e^{-\int_t^s c(\tau, X_\tau) d\tau} f(s, X_s) ds \middle| \mathcal{F}_t \right]. \quad (14)$$

For $(t, x) \in [0, T] \times \mathbb{R}^d$, using $X_t = x$ as the initial condition of the forward SDE (3) on the time interval $[t, T]$ *instead of* $X_0 = \xi$, the traditional Feynman–Kac formula [3] is recovered,

$$u(t, x) = \mathbb{E} \left[e^{-\int_t^T c(s, X_s) ds} g(X_T) - \int_t^T e^{-\int_t^s c(\tau, X_\tau) d\tau} f(s, X_s) ds \middle| X_t = x \right]. \quad (15)$$

For a general parabolic equation with a nonlinear function $\phi(s, x, u, \nabla u)$, we have

$$Y_t = \mathbb{E} \left[g(X_T) - \int_t^T \phi(s, X_s, Y_s, Z_s) ds \middle| \mathcal{F}_t \right],$$

and for given $(t, x) \in [0, T] \times \mathbb{R}^d$, the following nonlinear equation for $u(t, x)$ is obtained

$$u(t, x) = \mathbb{E} \left[g(X_T) - \int_t^T \phi(s, X_s, u(s, X_s), \nabla u(s, X_s)) ds \middle| X_t = x \right]. \quad (16)$$

3 FBSDE based neural network algorithms for quasi-linear parabolic PDEs

The learning of the solution will be based on the sample paths of the FBSDEs, which are link to the the PDE solution as in (5). Paths of the FBSDEs will be produced by a time discretization algorithm with samples of the Brownian motion W_t .

Let $0 = t_0 < \dots < t_N = T$ be a uniform partition of $[0, T]$. On each interval $[t_n, t_{n+1}]$, define time and Brownian motion increments as

$$\Delta t_n = t_{n+1} - t_n, \quad \Delta W_n = W_{t_{n+1}} - W_{t_n}. \quad (17)$$

Denoting X_{t_n} , Y_{t_n} and Z_{t_n} as X_n , Y_n and Z_n , respectively, by the Euler-Maruyama scheme to the FBSDEs (3) and (4), respectively, we have

$$X_{n+1} \approx X_n + \mu(t_n, X_n, Y_n, Z_n) \Delta t_n + \sigma(t_n, X_n, Y_n) \Delta W_n, \quad (18)$$

$$Y_{n+1} \approx Y_n + \phi(t_n, X_n, Y_n, Z_n) \Delta t_n + Z_n^T \sigma(t_n, X_n, Y_n) \Delta W_n. \quad (19)$$

Due to the relationship with the original parabolic PDE, in the above iterations, the solution to the parabolic PDE provides an alternative approach for Y_{n+1} and Z_{n+1} ,

$$Y_{n+1} = u(t_{n+1}, X_{n+1}), \quad (20)$$

$$Z_{n+1} = \nabla u(t_{n+1}, X_{n+1}). \quad (21)$$

In this paper, fully connected networks of L hidden layers will be used, which are given in the following formula

$$f_{\theta}(\mathbf{x}) = \mathbf{W}^{[L-1]} \sigma \circ (\dots (\mathbf{W}^{[1]} \sigma \circ (\mathbf{W}^{[0]}(\mathbf{x}) + \mathbf{b}^{[0]}) + \mathbf{b}^{[1]}) \dots) + \mathbf{b}^{[L-1]}, \quad (22)$$

where $W^{[1]}$ to $W^{[L-1]}$ and $b^{[1]}$ to $b^{[L-1]}$ are the weight matrices and bias unknowns, denoted collected by θ , respectively, to be optimized via the training, $\sigma(x)$ is the activation function and \circ implies the application of the activation function $\sigma(x)$ applied to a vector quantity component-wisely.

3.1 Existing FBSDE based neural networks algorithms

3.1.1 Deep BSDE from [7]

The Deep BSDE trains a network to approximate the random value Y_N at time $t = T$, where $X_0 = \xi$ is the input. Y_0, Z_0 are trainable variables and Y_0 is the desired quantity of the algorithm. $W_n, X_n, 0 \leq n \leq N$ are obtained from other function calls.

1. The initial value $X_0 = \xi$ is given. Trainable variables Y_0 and Z_0 are randomly initialized.
2. On each time interval $[t_n, t_{n+1}]$, use the Euler–Maruyama scheme for X_{n+1} and Y_{n+1} as in (18) and (19). Then, train a fully connected feedforward network $f_\theta^{(n+1)}(\cdot)$ such that for

$$X_{n+1} \mapsto Z_{n+1} = \nabla u(t_{n+1}, X_{n+1}) \approx f_\theta^{(n+1)}(X_{n+1}) \quad (23)$$

where $f_\theta^{(n+1)}(\cdot)$ is a fully connected neural network of the form of H hidden layers given in (22) and activation functions with ReLU, Tanh, Sigmoid, etc. have been tested.

3. Connect all quantities (subnetworks $f_\theta^{(n)}(\cdot)$, etc) at t_n to form a network that outputs Y_N , which is expected to be an approximation of $u(t_N, X_N)$.
4. The loss function is defined by a Monte Carlo approximation of

$$\mathbb{E} \|Y_N - g(X_N)\|^2. \quad (24)$$

The Deep BSDE has been shown to give convergent numerical results for various high dimensional parabolic equations [7] and a posteriori estimate suggests strong convergence of half order [10].

Remark 1. As the Deep BSDE method from [7] trains the network for the specific initial data $X_0 = \xi$ and only approximation to the PDE solution $Y_0 = u(0, \xi)$ is obtained. Once the desired initial data is changed, a new training may have to be carried out. Also, the total size of N individual sub-networks used to approximate $Z_n = \nabla u(t_n, X_n)$, $n = 1, \dots, N$ will grow linearly in terms of time discretization steps N , resulting in large amount of training parameter if higher accuracy of the PDE solution is desired.

3.1.2 FBSNNs from [8] (Scheme 1)

The FBSNNs trains a network $u_\theta(t, x)$ that directly approximates the solution to the PDE (1) in a region in the (t, x) space, with a fixed size in terms of number of hidden layers and neurons per layer.

1. The initial value $X_0 = \xi$ is given. Get Y_0 and Z_0 from the network

$$Y_0 = u_\theta(t_0, X_0), \quad Z_0 = \nabla u_\theta(t_0, X_0). \quad (25)$$

The gradient above is calculated by the automatic differentiation.

2. On each time interval $[t_n, t_{n+1}]$, use the Euler–Maruyama scheme (18) to calculate X_{n+1} , and use the network for Y_{n+1} and Z_{n+1} , i.e.

$$\begin{aligned} X_{n+1} &= X_n + \mu(t_n, X_n, Y_n, Z_n)\Delta t_n + \sigma(t_n, X_n, Y_n)\Delta W_n, \\ Y_{n+1} &= u_\theta(t_{n+1}, X_{n+1}), \\ Z_{n+1} &= \nabla u_\theta(t_{n+1}, X_{n+1}). \end{aligned} \quad (26)$$

Also calculate a reference value Y_{n+1}^\star using the Euler–Maruyama scheme (19)

$$Y_{n+1}^\star = Y_n + \phi(t_n, X_n, Y_n, Z_n)\Delta t_n + Z_n^T \sigma(t_n, X_n, Y_n)\Delta W_n. \quad (27)$$

3. The loss function is taken as a Monte Carlo approximation of

$$\mathbb{E} \left[\sum_{n=1}^N \|Y_n - Y_n^\star\|^2 + \|Y_N - g(X_N)\|^2 + \|Z_N - \nabla g(X_N)\|^2 \right]. \quad (28)$$

In this paper, in order to compare the training results using different values of N , the loss function for Scheme 1 is modified as

$$\begin{aligned} L_1[u_\theta; \xi] &= \frac{1}{M} \left[\sum_{\omega} \frac{1}{N} \sum_{n=1}^N \|Y_n - Y_n^\star\|^2 + \beta_1 \|Y_N - g(X_N)\|^2 \right. \\ &\quad \left. + \beta_2 \|Z_N - \nabla g(X_N)\|^2 \right] \end{aligned} \quad (29)$$

where M serves as the batch size of the training and ω denotes any instance of sampling of the discretized Brownian motion $W_n, 0 \leq n \leq N$, and β_1, β_2 are the penalty parameters for the terminal condition. The averaging factor $1/N$ is introduced for consistency consideration as the reduction of the loss function as N increases, when applied to the exact solution, is expected.

Remark 2. The FBSNNs algorithm proposed in [8] relies on a loss function involving the difference between sequences $\{Y_n\}$ and $\{Y_n^*\}$, which carries the information inside the time interval $[0, T]$. While the discrete random process $\{Y_n\}$ can be expected to approach a continuous stochastic process as defined in the backward SDE (4), the question whether the discrete sequence of random numbers $\{Y_n^*\}$ will converge to the same stochastic process is not clear. As a result, the question of the rate and extent for the difference between $\{Y_n\}$ and $\{Y_n^*\}$, thus the loss function, approaching to zero is not certain. Our numerical test will provide some evidence for this concern.

3.2 FBSDE based deep neural network algorithms for PDEs

In this section, we propose improved algorithms for the FBSDEs based deep neural networks similar to the approach in [8], but are mathematically consistent in the definition of the loss function and the discretization of both forward and backward SDEs related to the PDE solutions. Specifically, the loss will be made of the difference of two discrete stochastic processes, which will approach the same process given by the backward SDEs if the overall scheme converges.

3.2.1 FBSDE based algorithms - Scheme 2

Based on the Remark 2 from Section 3.1.2, we would like to design a new scheme whose loss function is expected to show the strong convergence rate of the Euler–Maruyama scheme for the discretization of the FBSDEs. A key factor will be to make the loss function as the pathwise differences between two stochastic processes, which will converge to the same continuous adapted diffusion processes if the time discretization of FBSDEs and DNN approximations converge.

Scheme 2. Train a DNN $u_\theta(t, x)$ to approximate the solution $u(t, x)$ of the parabolic PDE (1).

1. Given $X_0 = \xi$ and let $Y_0 = u_\theta(t_0, X_0)$, $Z_0 = \nabla u_\theta(t_0, X_0)$.
2. On each time interval $[t_n, t_{n+1}]$, calculate X_{n+1} and Y_{n+1} using the Euler–Maruyama scheme (18) and (19), respectively, and calculate Z_{n+1} using the network, i.e.

$$\begin{aligned} X_{n+1} &= X_n + \mu(t_n, X_n, Y_n, Z_n)\Delta t_n + \sigma(t_n, X_n, Y_n)\Delta W_n, \\ Y_{n+1} &= Y_n + \phi(t_n, X_n, Y_n, Z_n)\Delta t_n + Z_n^T \sigma(t_n, X_n, Y_n)\Delta W_n, \\ Z_{n+1} &= \nabla u_\theta(t_{n+1}, X_{n+1}). \end{aligned} \tag{30}$$

Then, calculate a reference value by the DNN representation of the PDE solution,

$$Y_{n+1}^* = u_\theta(t_{n+1}, X_{n+1}). \quad (31)$$

3. For a batch size M with ω denoting any of the M sample paths, the loss function is given as

$$L_2[u_\theta; \xi] = \frac{1}{M} \sum_{\omega} \left[\frac{1}{N} \sum_{n=1}^N \|Y_n - Y_n^*\|^2 + \beta_1 \|Y_N^* - g(X_N)\|^2 + \beta_2 \|Z_N - \nabla g(X_N)\|^2 \right], \quad (32)$$

where β_1, β_2 are the penalty parameters of the terminal condition.

The reference value Y_N^* is used in the terminal term in the loss function $L_2[u_\theta; \xi]$, because here it is a straightforward output of the neural network u_θ .

3.2.2 FBSDE based algorithms - Scheme 3

In the Scheme 2 above, the discrete process (31) is defined through the composite function using the DNN representation of the PDE solution $u_\theta(t, x)$. An alternative way is given below where both discrete processes are obtained from an Euler–Maruyama discretization of the SDEs.

Scheme 3: Train a DNN $u_\theta(t, x)$ to approximate the solution $u(t, x)$ of the parabolic PDE (1).

1. Given the initial values $X_0^{(1)} = X_0^{(2)} = \xi$ and we compute

$$Y_0^{(1)} = Y_0^{(2)} = u_\theta(t_0, \xi), \quad Z_0^{(1)} = Z_0^{(2)} = \nabla u_\theta(t_0, \xi) \quad (33)$$

from the network $u_\theta(t, x)$.

2. On each time interval $[t_n, t_{n+1}]$, calculate $X_{n+1}^{(1)}, Y_{n+1}^{(1)}$ and $Z_{n+1}^{(1)}$ as in (26) of

Scheme 1, then $X_{n+1}^{(2)}, Y_{n+1}^{(2)}$ and $Z_{n+1}^{(2)}$ as in (30) of Scheme 2, i.e.

$$\begin{aligned} X_{n+1}^{(1)} &= X_n^{(1)} + \mu(t_n, X_n^{(1)}, Y_n^{(1)}, Z_n^{(1)})\Delta t_n + \sigma(t_n, X_n^{(1)}, Y_n^{(1)})\Delta W_n, \\ Y_{n+1}^{(1)} &= u_\theta(t_{n+1}, X_{n+1}^{(1)}), \end{aligned} \quad (34)$$

$$Z_{n+1}^{(1)} = \nabla u_\theta(t_{n+1}, X_{n+1}^{(1)}), \quad (35)$$

$$\begin{aligned} X_{n+1}^{(2)} &= X_n^{(2)} + \mu(t_n, X_n^{(2)}, Y_n^{(2)}, Z_n^{(2)})\Delta t_n + \sigma(t_n, X_n^{(1)}, Y_n^{(1)})\Delta W_n, \\ Y_{n+1}^{(2)} &= Y_n^{(2)} + \phi(t_n, X_n^{(2)}, Y_n^{(2)}, Z_n^{(2)})\Delta t_n + (Z_n^{(2)})^T \sigma(t_n, X_n^{(2)}, Y_n^{(2)})\Delta W_n, \\ Z_{n+1}^{(2)} &= \nabla u_\theta(t_{n+1}, X_{n+1}^{(2)}). \end{aligned} \quad (36)$$

3. For a batch size M with ω denoting any of the M sample paths, the loss function is defined by

$$\begin{aligned} L_3[u_\theta; \xi] &= \frac{1}{M} \sum_{\omega} \left[\frac{1}{N} \sum_{n=1}^N \|Y_n^{(1)} - Y_n^{(2)}\|^2 + \beta_1 \left\| Y_N^{(1)} - g(X_N^{(1)}) \right\|^2 \right. \\ &\quad \left. + \beta_2 \left\| Z_N^{(1)} - \nabla g(X_N^{(1)}) \right\|^2 \right], \end{aligned} \quad (37)$$

where β_1, β_2 are the penalty parameters of the terminal condition.

4 Numerical results

In this section, we will test Scheme 1 from [8] and the new Scheme 2 and Scheme 3 for the following d -dimensional Black–Scholes–Barenblatt equation as the model problem: for $t \in [0, T]$ and $x \in \mathbb{R}^d$, the scalar function $u(t, x)$ satisfies

$$\begin{aligned} u_t &= -\frac{1}{2} \text{Tr} [\sigma^2 \text{diag}(X_t^2) \nabla \nabla u] + r(u - \nabla u \cdot x), \\ u(T, x) &= \|x\|^2. \end{aligned} \quad (38)$$

The PDE is corresponding to the FBSDEs

$$\begin{aligned} dX_t &= \sigma \text{diag}(X_t) dW_t, \\ X_0 &= \xi, \\ dY_t &= r(Y_t - Z_t \cdot X_t) dt + \sigma Z_t^T \text{diag}(X_t) dW_t, \\ Y_T &= g(X_T), \end{aligned}$$

where $g(x) = \|x\|^2$, and $\xi \in \mathbb{R}^d$ is the position where we demand the initial value $u(0, \xi)$. The exact solution to the PDE (38) is given by

$$u(t, x) = e^{(r+\sigma^2)(T-t)} \|x\|^2. \quad (39)$$

Parameters in our tests are given by $d = 100$, $T = 1.0$, $\sigma = 0.4$, $r = 0.05$ and

$$\xi = (1, 0.5, 1, 0.5, \dots, 1, 0.5). \quad (40)$$

In all the tests, we use a fully connected feedforward neural network for $u_\theta(t, x)$ with 5 hidden layers, each having 256 neurons. The activation function is the sine function as suggested by [8]. We train the network with the Adam optimizer with descending learning rates 1e-3, 1e-4, 1e-5, 1e-6 and 1e-7, for 20000, 30000, 30000, 10000 and 10000 steps, respectively. The batch size is $M = 8$.

In the loss functions (29), (32) and (37), the penalty parameters are chosen as $\beta_1 = \beta_2 = 0.02$.

Illustration of the training results in the high-dimensional space is provided along the sample paths. When training finishes, we use a finer time discretization with time steps $\Delta t_n = 1/1000$ for checking the accuracy. For $0 \leq n \leq 1000$, we calculate statistics of the relative error of this model problem at (t_n, X_n) (at $(t_n, X_n^{(2)})$ when using Scheme 3), which is defined by

$$e_n = \frac{\|u_\theta(t_n, X_n) - u(t_n, X_n)\|}{\|u(t_n, X_n)\|}. \quad (41)$$

1000 sample paths are generated to approximate the mean and the standard deviation (SD) of each e_n .

4.1 Scheme 1 from [8]

Fig. 1 shows the relative error of Scheme 1 for $N = 12, 48$ and 192 , where the mean error and the mean error plus two standard deviations of the error are shown. We can see the reduction of the errors from $N = 12$ to $N = 48$, however, the error increases from $N = 48$ to $N = 192$. This decrease of the accuracy is an indication that as the time discretization is refined, the two quantities in the definition of loss function (28) do not approach the same continuous stochastic process. In fact, as it is defined by (27), $\{Y_n^*\}$ may not converge to a continuous stochastic process at all.

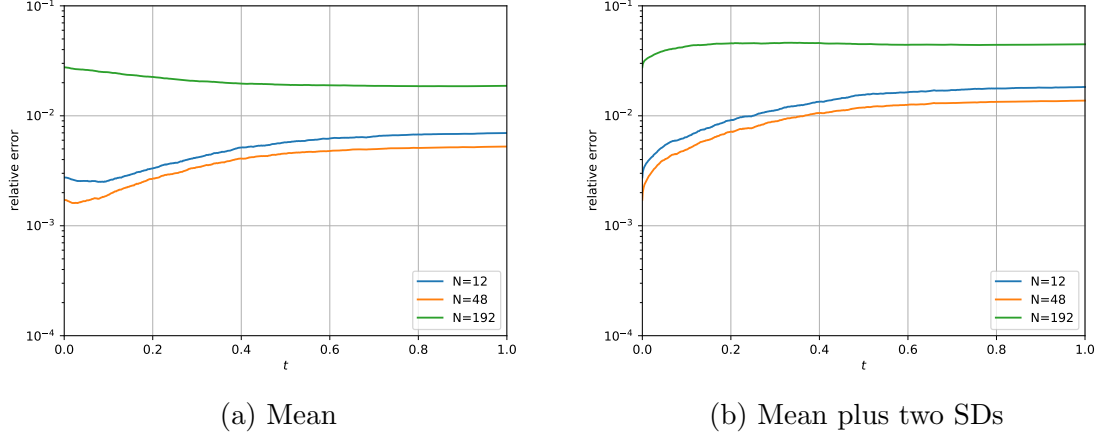


Figure 1: (Non-convergence) Relative error of Scheme 1 for $N = 12$ (middle), 48 (bottom) and 192 (top).

4.2 Scheme 2 and Scheme 3

Fig. 2 and Fig. 3 show the mean error and mean error plus two standard derivations of the error for Scheme 2 and Scheme 3 for $N = 12$, $N = 48$, $N = 192$ and $N = 768$, respectively.

The results in Fig. 2 and Fig. 3 show the convergence of the new Scheme 2 and Scheme 3 in contrast to the degeneracy of the accuracy of Scheme 1 when the time discretization is refined. For both new schemes, we can see improvement of the accuracy from $N = 48$ to $N = 192$ is close to the one from $N = 12$ to $N = 48$, but the improvement of $N = 768$ over $N = 192$ is a little less. This indicates the network training could dominate the error compared to the time discretization. Future research will be carried to improve the accuracy of the network for high dimensional solutions with the multiscale network proposed in [11].

Fig. 4 (a) (b) show the prediction of trained networks using Scheme 2 and Scheme 3 with $N = 192$ along eight sampled test paths depicted in Fig. 4 (c), in comparison with the exact solution where the average error of the prediction is given in Fig. 4 (d).

- Validity of trained network $u_\theta(t, x)$ in regions outside sampled training paths.

We are also interested in the verification of the trained networks in regions that are less likely to be sampled. Fig. 5 shows the results of the trained networks using

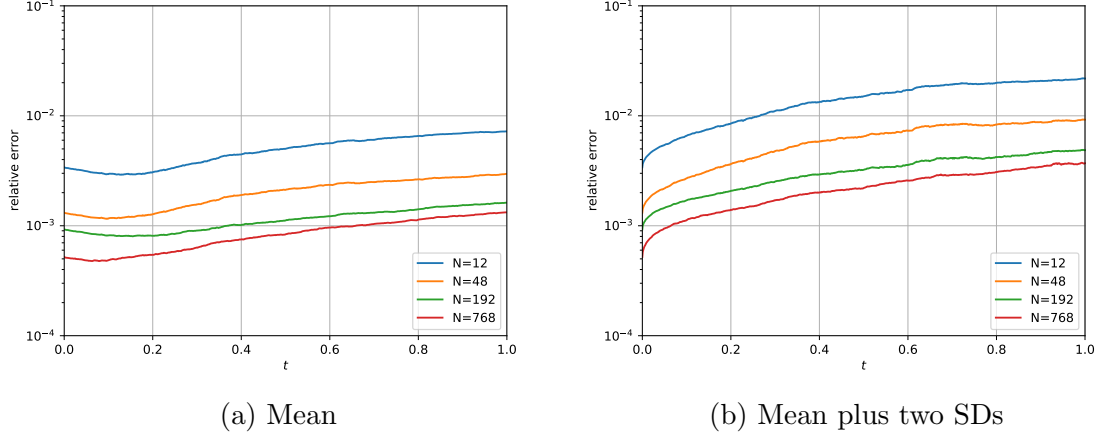


Figure 2: Relative error of Scheme 2 for $N = 12, 48, 192$ and 768 .

Scheme 2 over additional paths which originate from $X_0 = (1 + \epsilon)\xi$ with $\epsilon = 0.01$ and $\epsilon = 0.1$, i.e. 1% and 10% away from the starting point of the Brownian paths used in the training. As the sample paths pass through less trained regions, the accuracy of the prediction reduces but the averaged relative error still keeps within 1% for $\epsilon = 0.1$.

5 Conclusion

In this paper, we have proposed two FBSDE based DNN algorithms for high dimensional quasilinear parabolic equations. The key ingredient of our proposed algorithms lies in the fact that the loss function consists of, in addition to the terminal condition of the PDE, the path-wise difference of two convergent stochastic processes from either discretized SDEs or the PDEs network solution. As the two stochastic processes converges to the same stochastic processes in the Pardoux–Peng theory, the new algorithms are able to demonstrate closely the half-order strong convergence of the Euler–Maruyama scheme.

Future research will be done to improve the convergence of the networks and the overall schemes, and PDEs with more complicated and oscillatory solutions will be considered.

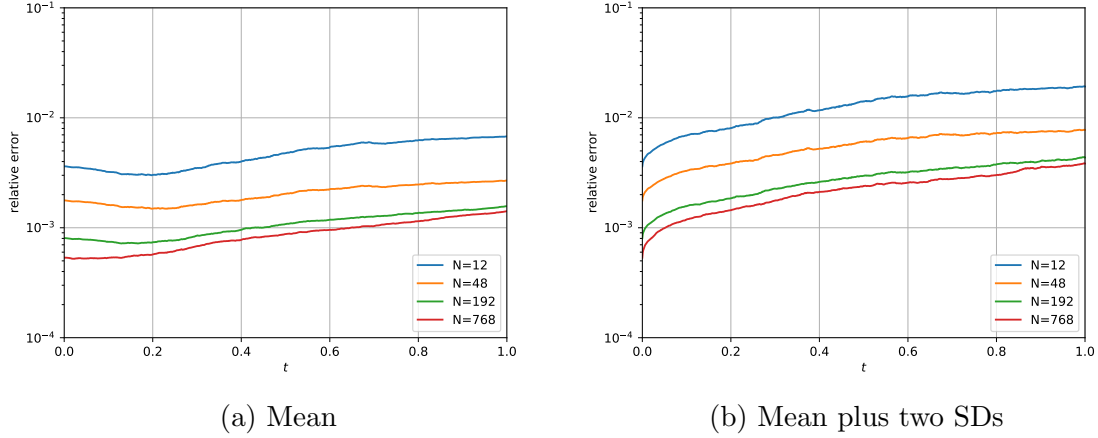
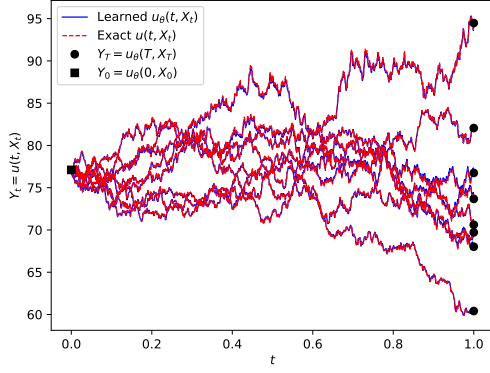


Figure 3: Relative error of Scheme 3 for $N = 12, 48, 192$ and 768 .

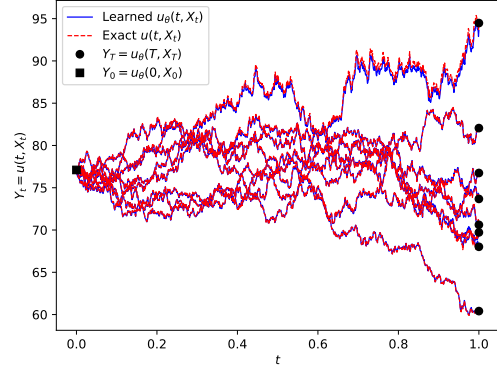
References

- [1] Doob JL. Classical potential theory and its probabilistic counterpart: Advanced problems. Springer Science & Business Media; 2012 Dec 6.
- [2] Pavliotis G, Stuart A. Multiscale methods: averaging and homogenization. Springer Science & Business Media; 2008 Jan 18.
- [3] Oksendal B. Stochastic differential equations. In Stochastic differential equations 2003 (pp. 65-84). Springer, Berlin, Heidelberg.
- [4] Pardoux E, Peng S. Backward stochastic differential equations and quasilinear parabolic partial differential equations. In Stochastic partial differential equations and their applications 1992 (pp. 200-217). Springer, Berlin, Heidelberg.
- [5] El Karoui N, Peng S, Quenez MC. Backward stochastic differential equations in finance. Mathematical finance. 1997 Jan;7(1):1-71.
- [6] Kloeden PE, Platen E. Numerical solution of stochastic differential equations. Springer Science & Business Media; 2013 Apr 17.
- [7] Han J, Jentzen A, Weinan E. Solving high-dimensional partial differential equations using deep learning. Proceedings of the National Academy of Sciences. 2018 Aug 21;115(34):8505-10.

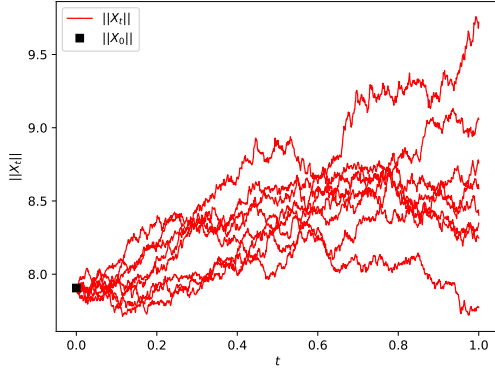
- [8] Raissi M. Forward-backward stochastic neural networks: Deep learning of high-dimensional partial differential equations. arXiv preprint arXiv:1804.07010. 2018 Apr 19.
- [9] Karatzas I, Shreve SE. Brownian Motion and Stochastic Calculus 1998 (pp. 47-127). Springer, New York, NY.
- [10] Han J, Long J. Convergence of the deep BSDE method for coupled FBSDEs. Probability, Uncertainty and Quantitative Risk. 2020 Dec;5(1):1-33.
- [11] Ziqi Liu, Wei Cai & Zhi-Qin John Xu, Multi-Scale Deep Neural Network (MscaleDNN) for Solving Poisson-Boltzmann Equation in Complex Domains. Communications in Computational Physics. 28(5), 1970-2001, 2020.



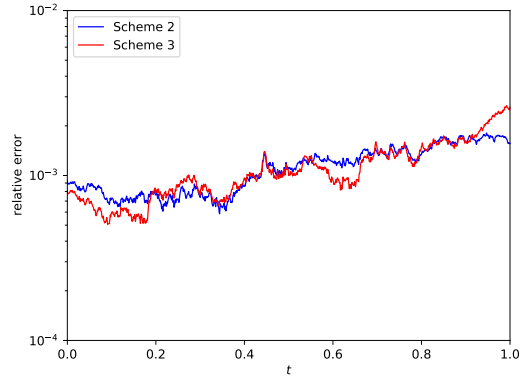
(a) Prediction of Scheme 2



(b) Prediction of Scheme 3

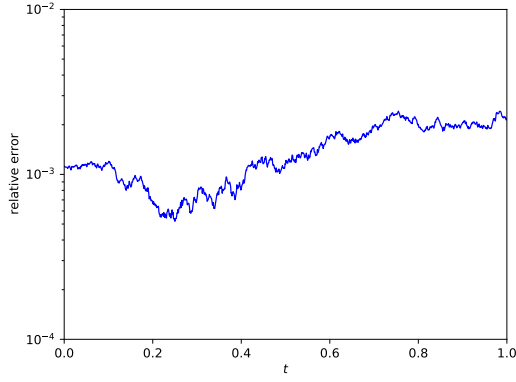


(c) $\|X_t\|$ along 8 sample paths

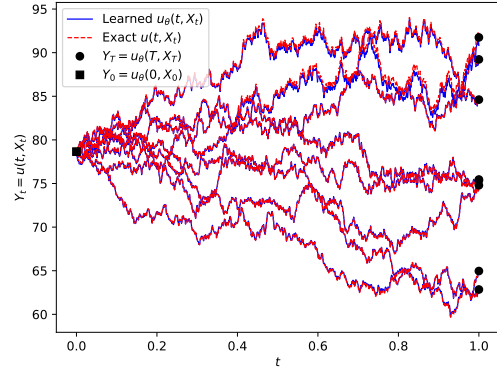


(d) Averaged relative error on $[0, T]$

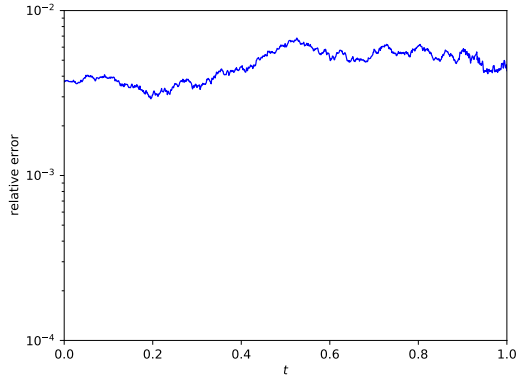
Figure 4: Prediction of 8 test sample paths from training results of Scheme 2 and Scheme 3, $N = 192$.



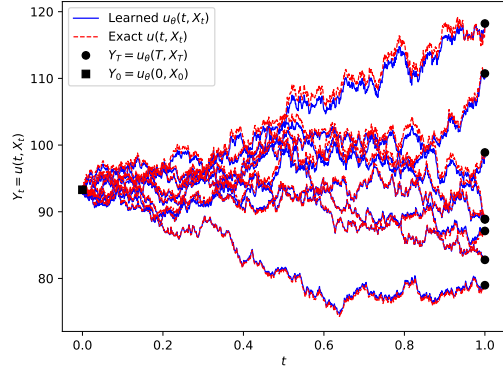
(a) Relative error, $\epsilon = 0.01$



(b) Sample paths, $\epsilon = 0.01$



(c) Relative error, $\epsilon = 0.1$



(d) Sample paths, $\epsilon = 0.1$

Figure 5: Prediction of trained network with Scheme 2, $N = 192$, along 8 test sample paths with shifted initial value $X_0 = (1 + \epsilon)\xi$.